Supplementary Information

In-Sensor Humidity Computing System for Contactless Human-Computer Interaction

*Meng Qi, Runze Xu, Guanglong Ding, Kui Zhou, Shirui Zhu, Yanbing Leng, Tao Sun, Ye Zhou, and Su-Ting Han**

Note 1: Discussion of the humidity sensitivity and fast response estimated.

The humidity sensitivity S can be estimated by the following equation[1]

$$Z_c = 1 / (j\omega C)$$

$$S = C_{RH} / C_0 \times 100\% \quad (1)$$

where Z_c represents the complex impedance of the capacitor, ω is the angular frequency, C_{RH} is the capacitance at certain humidity levels and C_0 is the capacitance at the initial humidity level. The certain and initial RH are 90% and 40%, respectively.

The response time is estimated by calculating dI/dt, which is the derivative of the response current versus time.[2] That is to say that the time required to reach the maximum value from 0.

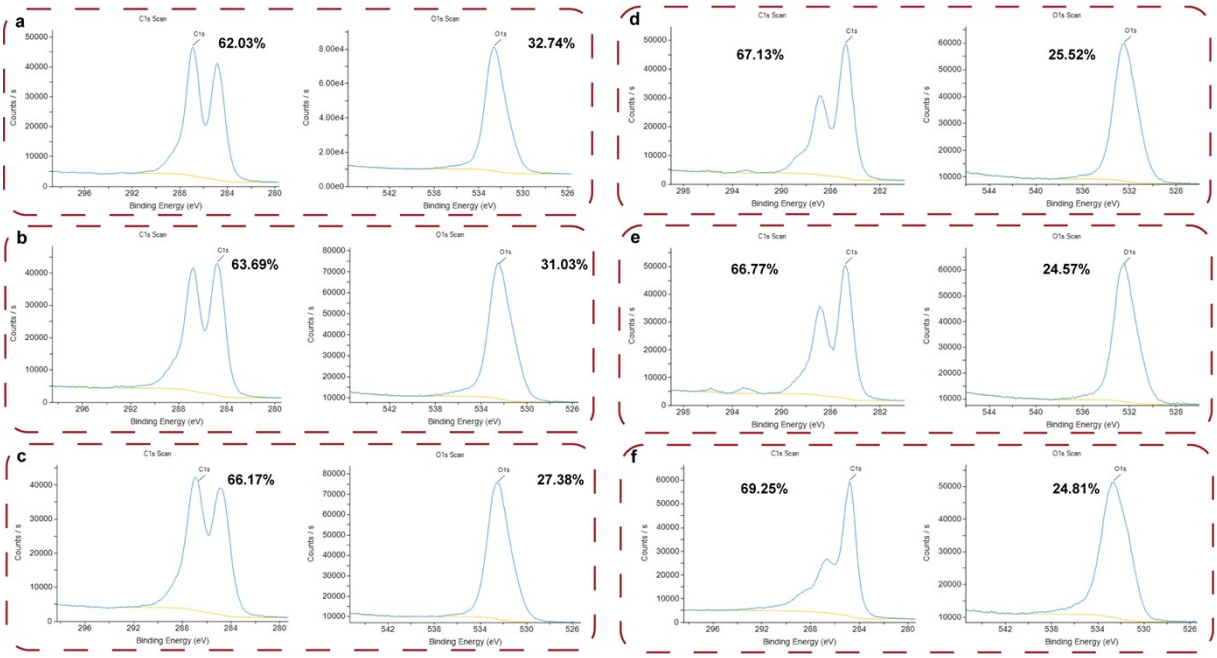

Figure S1. The XPS C 1s and O1s core-level spectrum of the as-deposited GO planar structure with different distances from the TE (the a is adjacent to the TE and the f is away from the TE).

We performed the stability and reliability test of the Ti/GO/HfO_x/Pt device, the statistical data was shown in Figure S2. The relative fluctuations of the V_{SET}/V_{RESET} (HRS/LRS) were calculated by the standard deviations (σ)/mean value (μ), which is acceptable variability in resistive switching for different humidity levels.

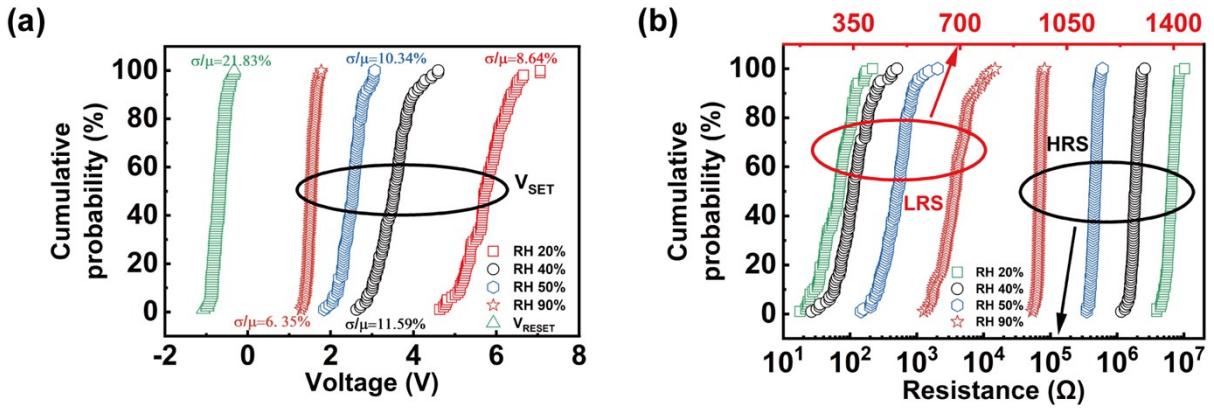

Figure S2. Statistical performance of the (a) voltage and (b) resistance for different humidity levels.

We have further performed the experiment on the synaptic behaviors, which is estimated by applying voltage pulses with different amplitude and time interval, as shown in Figure S3. The conductance was read at 0.6 V after each pulse. It can be seen that a typical characteristic of synaptic behaviors can be also obtained by electrical testing.

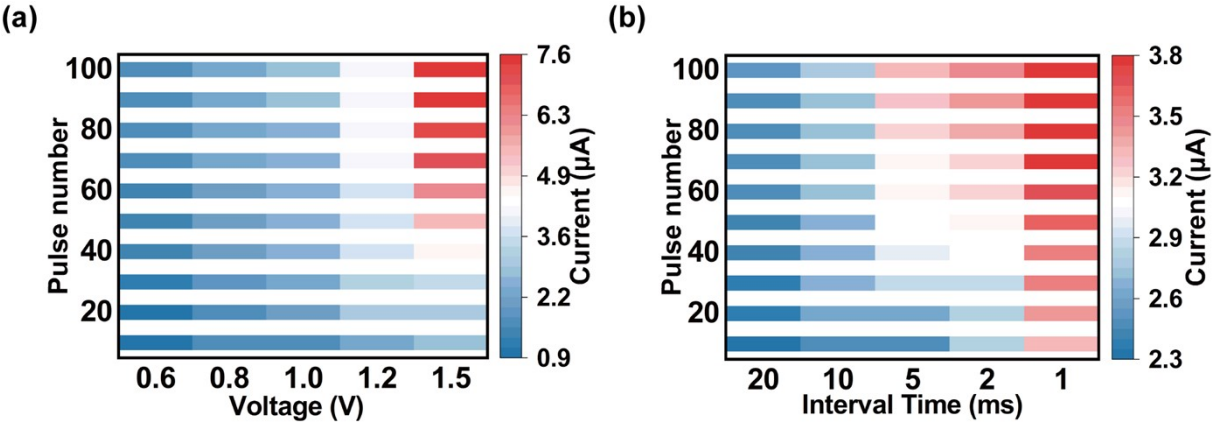

Figure S3. The current variation of the GO/HfO_x memristor at various (a) voltage pulse amplitude and (b) interval time.

Figure S4 shows the excitatory postsynaptic current (EPSC) inspired, which underlie ΔW variation. The fitting details of the PPF curve could be fitted by a double exponential function:[3-5]

$$PPF = C_1 \exp(-t/\tau_1) + C_2 \exp(-t/\tau_2) \quad (2)$$

where t is the Δt, C_1 and C_2 are the initial facilitation magnitudes of the respective phases, the τ_1 (rapid phase) and τ_2 (slow phase) are the characteristic relaxation times of forgetting process. In the fitting, τ_1 and τ_2 are 2.67 and 588.01 ms, and the parameters C_1 = 41.88%, C_2 = 4.13%. The time scale of our electronic synapses is comparable to that of biological synapses.

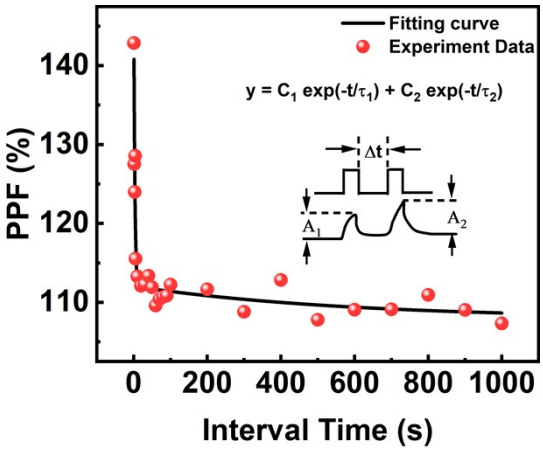

Figure S4. The variation of PPF index with the voltage pulse pair interval.

Note 2: Discussion of the nonlinearity calculated.

The nonlinearity A can be calculated by the following equation[6,7]

$$G = G_{min} + B\,(1 - \exp(-AP)) \qquad (3)$$

where C_{RH} is the conductivity value during the potential process, G_{min} is the minimum value among them, P is the normalized number of pulses, B is the fitting constant and the value of A is the nonlinearity of LTP curves.

Note 3: Discussion of the conjugate gradient algorithm.

For the conjugate gradient algorithm, the step is adjusted in each iteration. The detailed algorithm is as follows:[8]

the conjugate gradient algorithm is started by searching along the steepest descent direction at the first iteration:

$$p_0 = -g_0$$

then perform a line search to determine the best distance to move in the current search direction:

$$x_{k+1} = x_k + \alpha_k p_k$$

the new search direction conjugated to the previous search direction is then determined by combining the new steepest descent direction with the previous direction:

$$p_k = -g_k + \beta_k p_{k-1}$$

the various forms of conjugate gradients are distinguished by the calculation of the constant β_k. The update program for Fletcher Reeves is as follows:

$$\beta_k = \frac{g_k^T g_k}{g_{k-1}^T g_{k-1}}$$

The high network recognition rate is related to the noise of dataset. In the training of neural networks, the noise dataset is used for training to enhance the reliability of neural network handwriting letter recognition and classification. The weighted data with partial noise is shown in Figures S5. The results demonstrated an acceptable accuracy for handwriting letter recognition and classification.

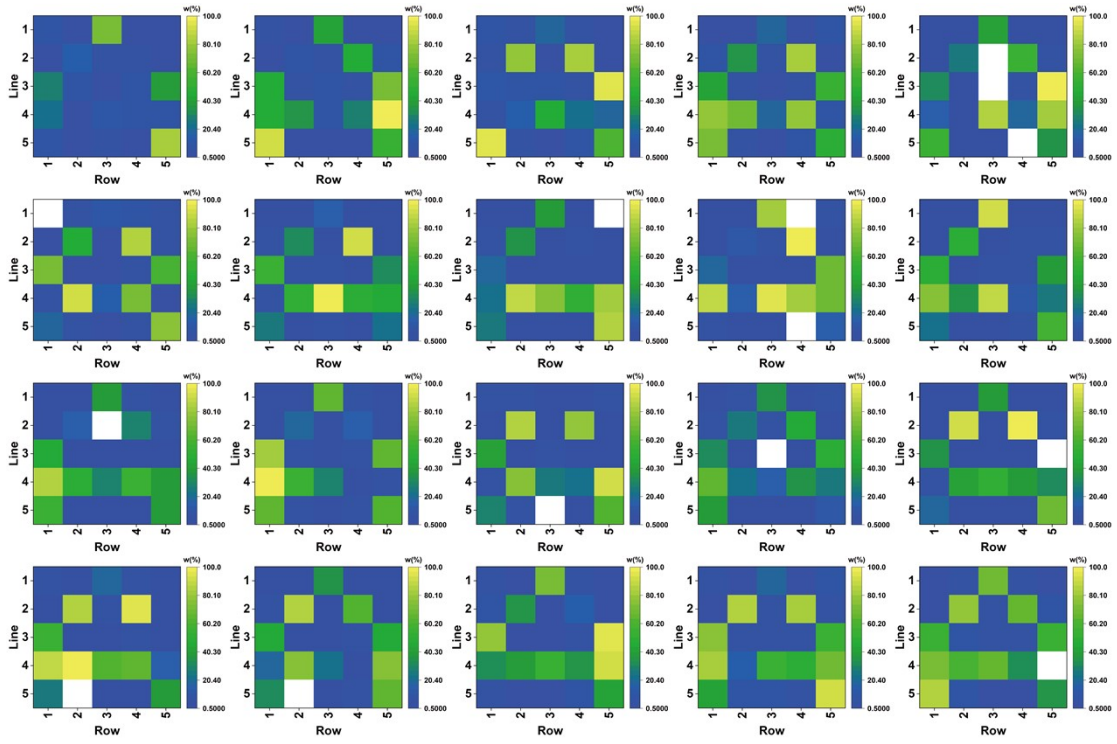

Figure S5. Part of the training data set with letter “A”.

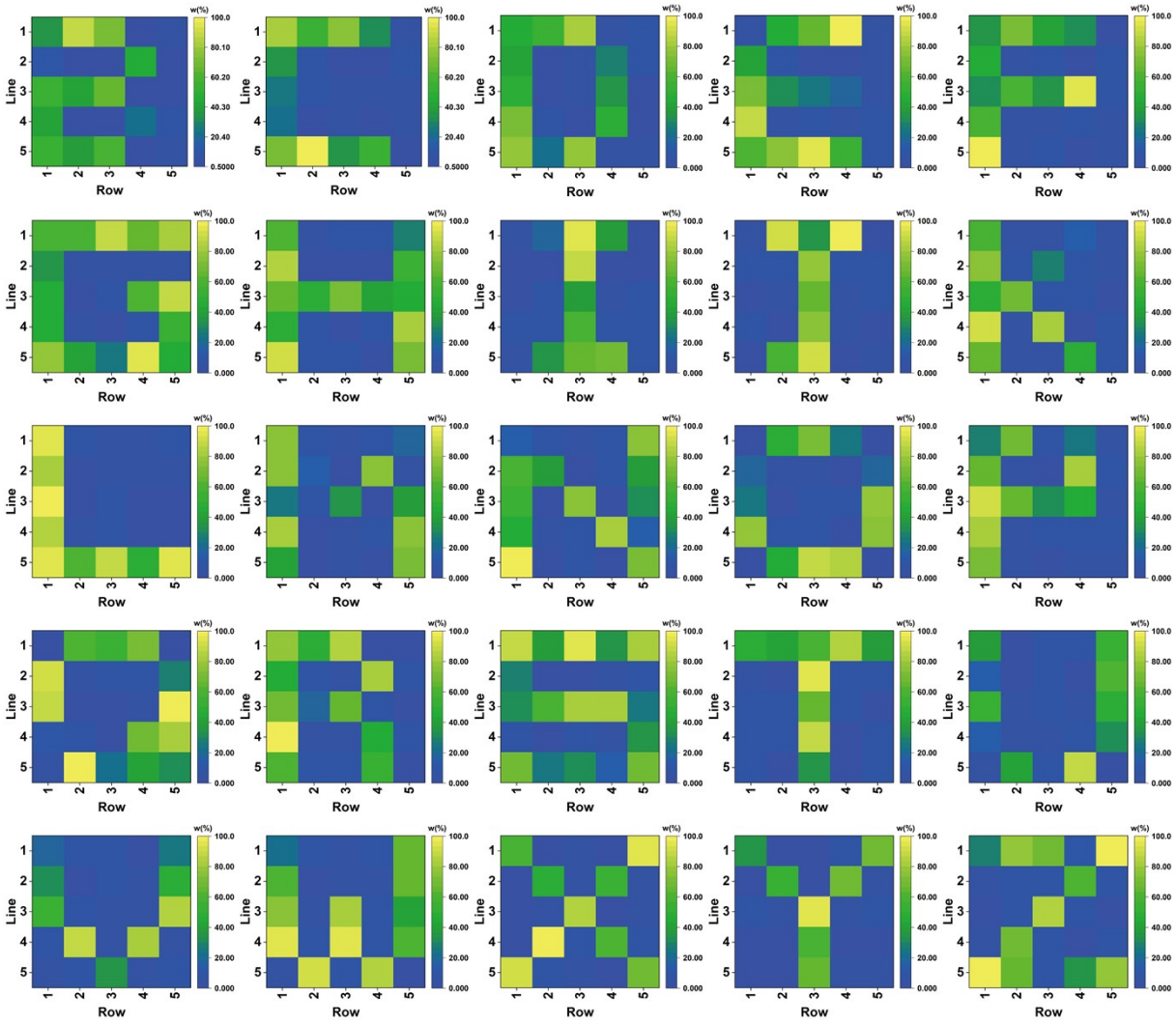

Figure S6. The weight of humidity-memristive synapse 5 × 5 array after handwriting (Handwritten letters B-Z).

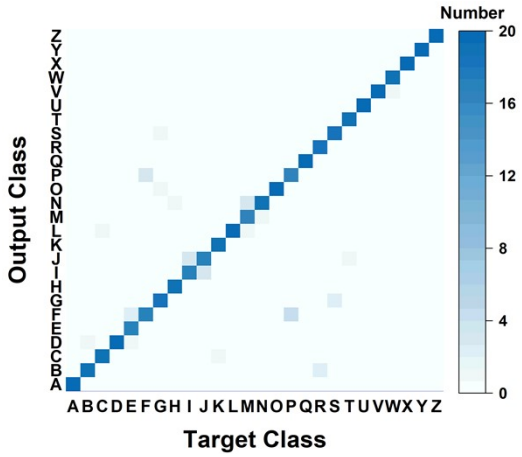

Figure S7. Confusion graph of the output class and the target class about handwriting letters of alphabet 'A' – 'Z' after 40 cycles.

References

1 Z. Song, S. Li, B. Hou, Z. Cheng, Y. Xue and B. Chen, *IEEE Sensors Journal*, 2023, **23**, 2291-2302.

2 S. Li, Y. Zhang, X. Liang, H. Wang, H. Lu, M. Zhu, H. Wang, M. Zhang, X. Qiu, Y. Song and Y. Zhang, *Nat. Commun.*, 2022, **13**, 5416.

3 K. Wang, J. Liu, M. E. El-Khouly, X. Cui, Q. Che, B. Zhang and Y. Chen, *ACS Appl. Mater. Interfaces*, 2022, **14**, 36987-36997.

4 Z. Li, B. Zhang and Y. Chen, *Organic Electronics*, 2022, **102**, 106447.

5 Z. Zhao, Q. Che, K. Wang, M. E. El-Khouly, J. Liu, Y. Fu, B. Zhang and Y. Chen, *iScience*, 2022, **25**, 103640.

6 J. Lee, B. H. Jeong, E. Kamaraj, D. Kim, H. Kim, S. Park and H. J. Park, *Nat. Commun.*, 2023, **14**, 5775.

7 M. Farronato, P. Mannocci, M. Melegari, S. Ricci, C. M. Compagnoni and D. Ielmini, *Adv. Mater.*, 2022, **35**, 2205381.

8 T.-T. Yao, Z.-J. Bai and Z. Zhao, *Numer Linear Algebra. Appl.*, 2019, **26**, e2221.